JOURNAL OF COLLOID AND INTERFACE SCIENCE **185,** 57–67 (1997)
ARTICLE NO. CS964581

Shear-Thickening Response of Fumed Silica Suspensions under Steady and Oscillatory Shear

SRINIVASA R. RAGHAVAN AND SAAD A. KHAN[1]

Department of Chemical Engineering, North Carolina State University, Raleigh, North Carolina 27695-7905

Received March 14, 1996; accepted September 3, 1996

Suspensions of fumed silica in polypropylene glycol exhibit shear-thickening under steady shear and "strain-thickening" under oscillatory shear. Strain-thickening refers to a sharp increase in the complex viscosity η^* observed at critical combinations of strain-amplitude and frequency. Two regimes of strain-thickening behavior have been found: The first occurs at high critical strains and low frequencies, whereas the second occurs at high critical frequencies and a constant lower strain. Strain-thickening in the first regime can be explicitly correlated with steady shear-thickening, using a modified version of the Cox–Merz rule. Accordingly, strain-thickening data for the complex viscosity η^* as a function of the maximum dynamic shear-rate $\gamma_0\omega$ can be superposed against shear-thickening data for the steady viscosity as a function of the steady shear rate. Such a correlation between the two kinds of thickening phenomena has not been reported previously. The combination of shear- and strain-thickening behavior can be qualitatively explained using a clustering mechanism, which attributes the various phenomena to the formation of temporary, flow-induced clusters. The two regimes of strain-thickening are a result of differences in the relative ease of cluster formation.

Key Words: **shear-thickening; strain-thickening; suspensions; rheology; fumed silica.**

1. INTRODUCTION

The shear-thickening behavior of concentrated dispersions has been a major topic of interest for rheologists over the last two decades (1–4). The term *shear-thickening* is typically used to refer to the increase in apparent viscosity when the applied shear rate is increased. The phenomenon is frequently encountered during the processing of concentrated dispersions in various industries.

The onset of shear-thickening marks the point when hydrodynamic interactions begin to predominate in the system (3, 4). However, the microstructural basis for this phenomenon still remains unresolved. Hoffman, in his pioneering studies, used a combination of rheology with *in situ* light diffraction to elucidate microstructural changes that occur during shear-thickening (1, 2). He concluded that the incipience of shear-thickening at a critical shear rate $\dot{\gamma}_c$ corresponds to a transition from an easy flowing state where the particles are ordered into layers to a disordered state where this ordering is absent. This mechanism is generally called an *order-disorder transition.*

Subsequent researchers have questioned whether an order-disorder transition indeed takes place in all shear-thickening systems. Stokesian dynamics simulations have shown that the shear-thickened state is characterized by clusters of particles (5–8). The formation of these flow-induced clusters results in an increased dissipation of energy and, consequently, the viscosity increases. Thus, according to these researchers, shear-thickening is not related to the destruction of ordered layers but to the generation of particle clusters. It should be noted that under certain conditions both events may occur simultaneously (i.e., the disruption of the ordered layer structure can be caused by the clustering of particles). However, for the clustering theory to hold, it is not at all necessary to assume the existence of an ordered state before the shear-thickening transition. Further evidence for the clustering hypothesis has been provided recently by the work of Bender and Wagner, through optical dichroism measurements (9, 10).

For a suspension to exhibit shear-thickening, two conditions must hold. Firstly, the volume fraction of solids in the suspension must be very high; in addition, the suspension must be nonflocculated (3, 4). The latter criterion requires that the particles be either neutral or repel one another by virtue of electrostatic, steric, or entropic interactions (3). Many experimental studies of shear-thickening have been performed on model suspensions of monodisperse spheres, stabilized by steric or electrostatic means (e.g., 4, 11). Most of the experimentation involved steady shear rheology.

Very few researchers have investigated the dynamic rheological properties of shear-thickening dispersions. The linear viscoelastic response of such dispersions typically shows sol-like behavior: the elastic (G') and viscous (G'') moduli depend strongly on frequency, with G'' exceeding G' (12).

[1] To whom correspondence should be addressed. E-mail: khan@che.ncsu.edu.

0021-9797/97 $25.00

This is the expected response for such systems, as it reflects the nonflocculated nature of the dispersions. However, the viscoelastic response under nonlinear oscillatory conditions, involving large strain amplitudes, shows some remarkable features. It has been found that the moduli make an abrupt transition to higher levels when the strain amplitude and the frequency of the deformation exceed certain values (12–14). This phenomenon has been variously termed strain-thickening or flow-blocking. Independent observations of this phenomenon have also been made on solutions of associative polymers, although there is little published data for the same.

In this study, we report the shear-thickening as well as strain-thickening behavior of nonflocculated fumed silica suspensions. Fumed silica is an amorphous, nonporous silica prepared by a flame hydrolysis process (15, 16). Its primary structure consists of branched *aggregates* formed by the fusion of primary spherical particles of SiO_2. As a result of this complex aggregated structure, the silicas exhibit high surface areas (>100 m^2/g). The surface chemistry of fumed silica is hydrophilic due to the presence of hydroxyl groups on the surface. When dispersed in a nonpolar liquid, aggregates of silica can interact through hydrogen bonding of surface hydroxyls. This gives rise to larger structures called flocs, which can be further connected into a three-dimensional network. The formation of these structures leads to large increases in viscosity and gel-like behavior (17). However, if the liquid is polar, its molecules preferentially form hydrogen bonds with the surface hydroxyls present on the silica aggregates.

We have used a polar liquid, viz. poly(propylene glycol) (PPG) as the continuous phase in our study. The molecular weight of the glycol is low, and it is a low viscosity, Newtonian liquid. When fumed silica is dispersed in PPG, the silica aggregates preferentially interact with the glycol molecules. This leads to nonflocculated suspensions which exhibit low viscosity and frequency-dependent dynamic moduli. As mentioned earlier, these suspensions exhibit both shear- and strain-thickening. The present study is part of an ongoing investigation of various fumed silica-based systems in our laboratories. Fumed silica suspensions and gels are finding applications in state-of-the-art technologies such as for polymer electrolytes in lithium batteries (18).

2. MATERIALS AND METHODS

The fumed silica used was Aerosil D150 (Degussa Corporation, Akron, OH). This is a hydrophilic silica, with a specific surface area of ≈ 150 m^2/g and a primary spherical particle size of 14 nm. Fumed silica primary particles are irreversibly fused into larger structures called aggregates, that cannot be disrupted by shear. Figure 1 shows the branched chain-like structure of silica aggregates (19). In addition, the aggregates are found to be self-similar (i.e., fractals), with a characteristic fractal dimension d_f equal to 1.71 ± 0.05 in three-dimensional space. This value for d_f corresponds to diffusion-limited aggregation of the primary particles in the latter stages of flame hydrolysis (16, 19).

The continuous phase in our studies is a polypropylene glycol having an average molecular weight of 725 (Aldrich Chemicals). The viscosity of the PPG liquid under ambient conditions was ≈ 1.2 poise. Each suspension was prepared by adding the liquid to the silica in a blender and mixing for approximately 1 minute (17). Samples were made in batches of 60 ml and placed under vacuum at room temperature for about 12 h to remove air bubbles. The silica concentration in the suspension was varied between 3 and 10% (w/w basis).

Rheological experiments were carried out on a Rheometrics Mechanical Spectrometer (RMS-800). A cone-and-plate fixture having a cone angle of 0.04 radians and a diameter of 50 mm was used. At the higher fumed silica concentrations, the results were checked on a different cone-and-plate fixture having a cone angle of 0.1 radians and a diameter of 25 mm. The use of two different fixtures ensured that instrumental artifacts, such as wall slip, were absent.

Experiments were conducted under both steady as well as dynamic oscillatory shear. The steady-shear rate sweeps involved the measurement of the torque response at discrete shear rates in succession. At each shear rate, the sample was sheared for about 60 s before any data were collected. Step shear experiments showed that this time was sufficient for the attainment of steady state. Dynamic experiments were mainly twofold: strain sweeps, where the frequency was held fixed and the strain amplitude increased in discrete steps, and frequency sweeps performed at a constant strain, with the frequency being increased in discrete steps.

3. RESULTS

The linear viscoelastic response of a suspension of 10% fumed silica in PPG is shown in Fig. 2a. The elastic (G') and viscous (G'') moduli are seen to depend strongly on frequency, and G'' dominates over G'. For comparison, the linear response of a flocculated suspension of 5% fumed silica in mineral oil is shown in Fig. 2b (17). The mineral oil system exhibits a frequency-independent elastic modulus G' that is two orders of magnitude higher than the G' for the PPG system. This figure clearly indicates that the suspension in PPG is nonflocculated, with a microstructure composed of discrete units. Flocculation is prevented due to the adsorption of PPG chains on the silica aggregates, by means of hydrogen bonds between the hydroxyls on the silica surface and the hydroxyl end groups or the ether oxygens on the PPG.

The steady shear response of the glycol-based suspension is shown in Fig. 3. At low shear-rates, slight shear-thinning can be observed. The low level of viscosity at these shear

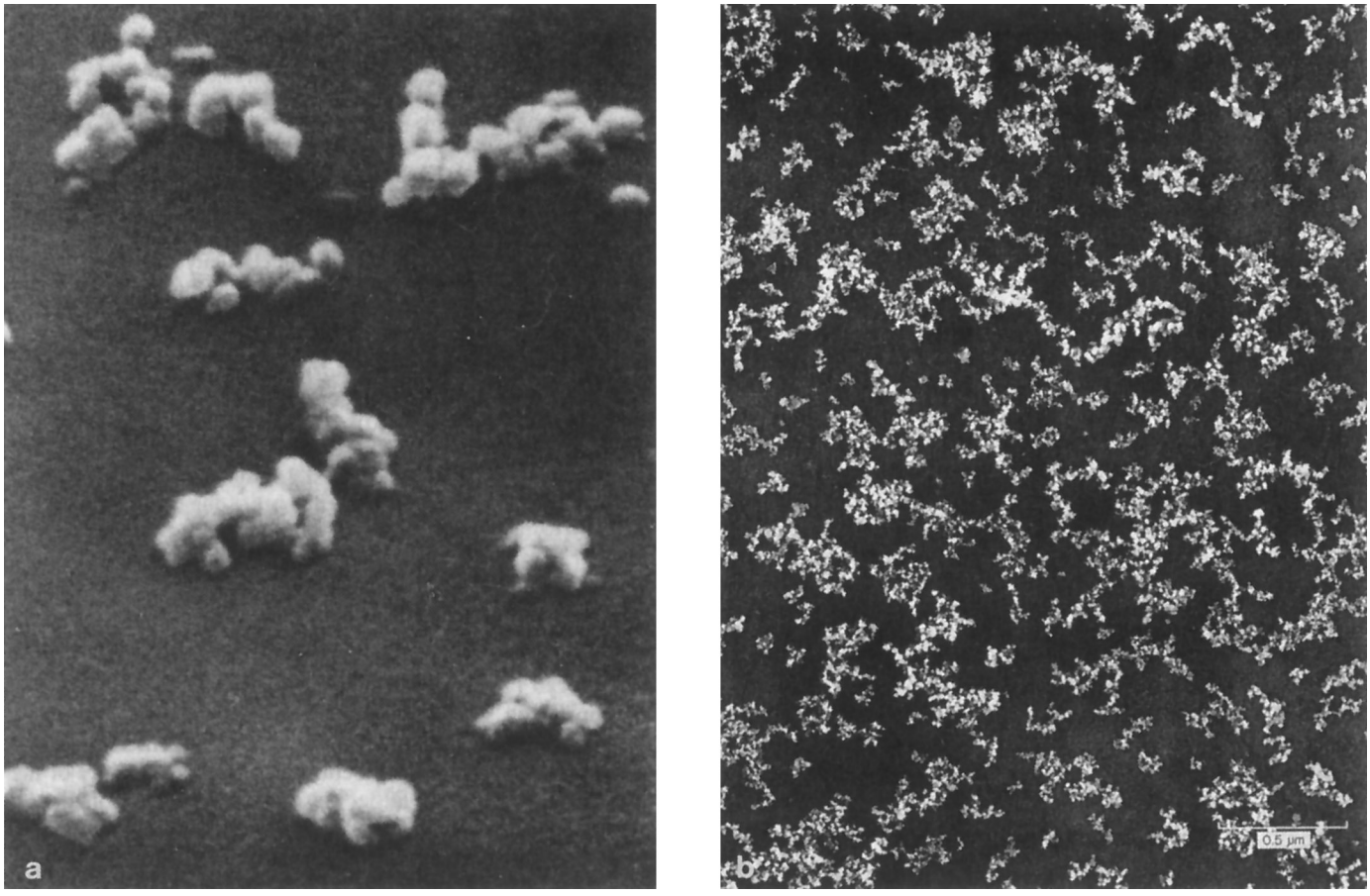

FIG. 1. (a) Micrograph (SEM) of gold-coated fumed silica *aggregates* indicating their chain-like structure. The aggregates are formed by the fusion of spherical primary particles (14 nm dia.). (b) Electron micrograph of fumed silica powder showing the fractal nature of the aggregates. Some mechanical agglomeration of the aggregates, which can be reversed on dispersion, is seen. The aggregates, however, cannot be disrupted into primary particles. Reproduced from Forsman *et al.* (19).

rates reflects the nonflocculated nature of the system. At a shear-rate $\dot{\gamma}$ close to 10 s^{-1} the viscosity begins to increase steeply until $\dot{\gamma} \approx 30\ s^{-1}$. The viscosity rises by nearly an order of magnitude in the process. At the point of incipience of shear thickening (which we will denote by $\dot{\gamma}_c$), we were able to detect normal stresses that continued to increase with shear-rate. These normal stresses were not reproducible unlike the flow curve and are hence not shown. Generally for

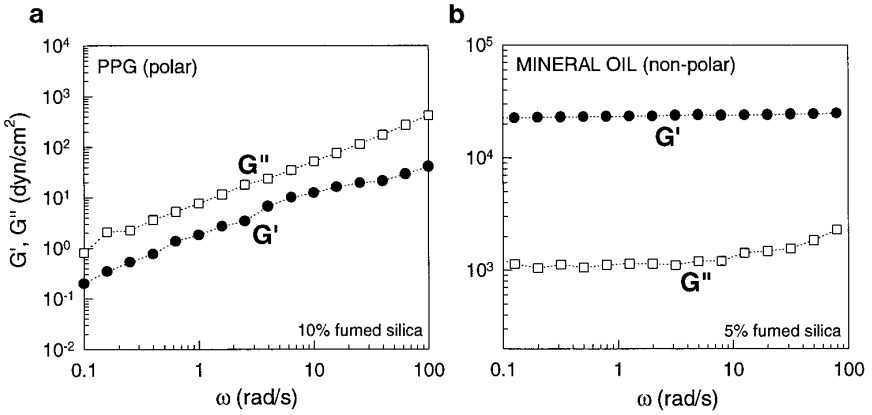

FIG. 2. Elastic G' and viscous G'' moduli as a function of frequency for two dispersions containing fumed silica. (a) refers to a suspension of 10% fumed silica in polar poly(propylene glycol) (PPG), while (b) corresponds to a 5% silica dispersion in non-polar mineral oil.

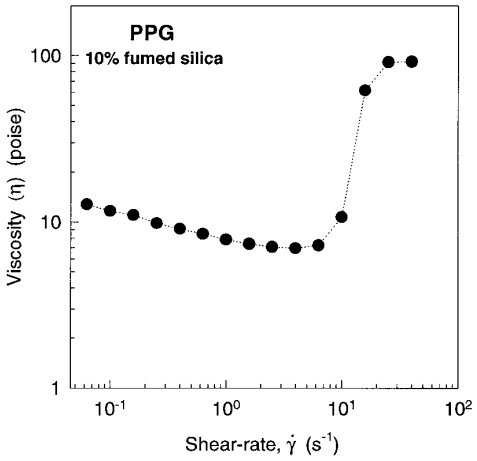

FIG. 3. Steady-shear viscosity as a function of shear-rate for a suspension of 10% fumed silica in poly(propylene glycol).

all the suspensions studied, the normal stresses were too low before $\dot{\gamma}_c$ and relatively high beyond $\dot{\gamma}_c$. Similar behavior of the normal stresses in shear-thickening systems, including their irreproducibility, has been cited by other workers (20).

Strain-Thickening Behavior under Dynamic Shear

The viscoelastic behavior of the 10% fumed silica suspension in PPG is illustrated in Fig. 4a in terms of a strain sweep. The experiment was performed from low to high amplitude strains at a constant frequency of 10 rad/s. Data are also shown in Fig. 4b for the mineral oil-based system, for which the elastic modulus G' is observed to be considerably greater than the viscous modulus G'' at low strain amplitudes. This behavior is characteristic of a flocculated gel and is consistent with the frequency response for the same system indicated earlier in Fig. 2b. Additionally, the G' for the gel decreases more rapidly with strain than G'' and ultimately falls below G''. In contrast, the nonflocculated suspension exhibits *strain-thickening* at high strain amplitudes, with both moduli G' and G'' showing an abrupt jump to higher levels at a particular strain (Fig. 4a).

Strain sweeps were conducted at several frequencies and are plotted in Fig. 5. In Fig. 5a, we show data for G' and in Fig. 5b, for the complex shear modulus $|G^*|$. The quantity $|G^*|$ is derived directly from the peak amplitude of the torque and is independent of the phase angle. An increase in $|G^*|$ thus corresponds to a larger torque response exerted by the sample—for this reason the preceding phenomenon has also been called flow-blocking in the literature (12). The data in Fig. 5 indicates that the transition to strain-thickening (flow-blocking) behavior occurs at smaller strains as the frequency of the deformation is increased.

The same strain-thickening phenomenon can also be demonstrated in a frequency sweep experiment where the strain amplitude of the deformation is kept constant and the frequency is increased. Figure 6a shows the frequency response at a strain of 750% along with the linear response depicted earlier in Fig. 2a for the same suspension. At a frequency of approximately 1 rad/s, the moduli make an abrupt transition to a higher level. The increase can also be observed in the complex viscosity η^* which is simply the complex modulus $|G^*|$ divided by the frequency of the deformation ω. The complex viscosity (Fig. 6b) offers a more dramatic evidence of strain-thickening, increasing steeply at the appropriate frequency. The increase in η^* is shown for two strain amplitudes, 500% and 750%.

The dramatic increase in $|G^*|$ or other derived rheological quantities at critical combinations of the amplitude and frequency is not an instrumental artifact. It is reproducible and has been verified on other geometries. We have found the effect to be reversible. For example, the same strain sweep data can be generated by decreasing the deformation successively in steps instead of increasing it. Moreover, contributions from higher harmonics to the nonlinear viscoelas-

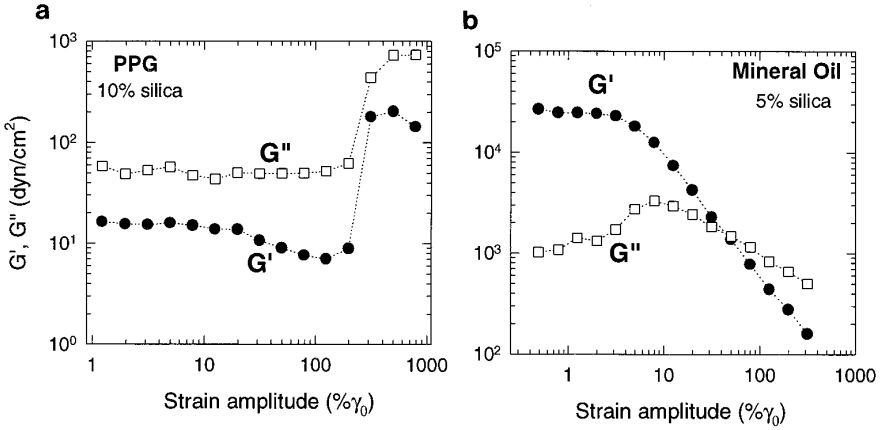

FIG. 4. Elastic G' and viscous G'' moduli as a function of strain amplitude for the same systems shown in Fig. 2. (a) corresponds to the 10% silica suspension in PPG, while (b) shows data for the 5% silica dispersion in mineral oil. Both experiments were performed at a frequency of 10 rad/s.

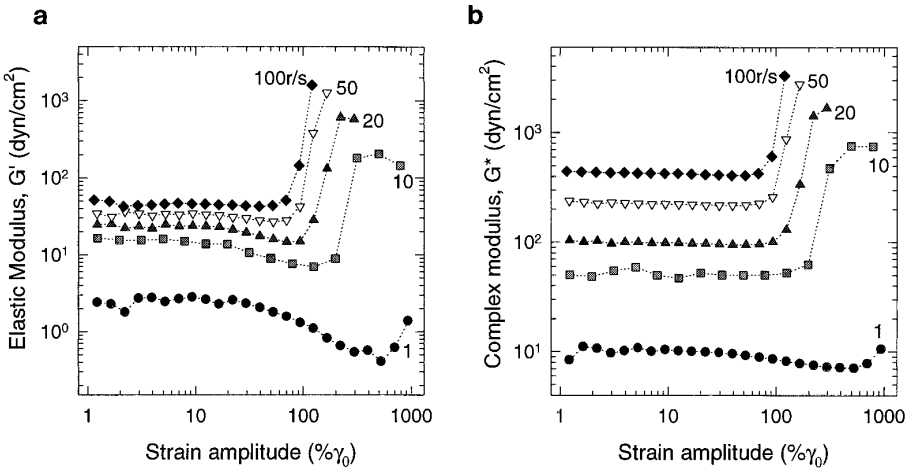

FIG. 5. Moduli as a function of strain amplitude for a 10% fumed silica suspension in PPG. The strain sweeps were conducted at different frequencies, each indicated beside the corresponding curve. In (a), data are shown for the elastic modulus G', and in (b) for the complex shear modulus G^*.

tic response appear to be negligible, indicating the strain-thickening to be a material phenomenon. We also conducted stress relaxation experiments immediately after subjecting the suspension to strain-thickening deformations. The stress was observed to decrease instantaneously, thereby indicating that structures formed during strain-thickening do not persist after the deformation is ceased.

Strain-thickening under oscillatory shear has been demonstrated in a few earlier studies on dispersions. Miller *et al.* (14) studied the rheology of rocket propellants, which exist as highly concentrated suspensions. They measured the dynamic moduli G' and G'' as a function of strain at a single frequency, viz. 5 rad/s. Both G' and G'' increased with strain amplitude for strains exceeding 10%. The authors interpreted the dynamic strain thickening as an order-disorder transition similar to that postulated by Hoffman (1, 2) for steady shear-thickening.

Laun *et al.* (13) reported the rheological behavior of concentrated dispersions consisting of monodisperse polymer latex particles in ethylene or diethylene glycol. Their oscillatory tests involved increasing the amplitude gradually at a given frequency. At a critical amplitude the dispersion became ''highly viscous.'' The authors did not specifically show data for the evolution of moduli with strain amplitude. However, they did show plots of the critical amplitude at which thickening was first observed, as a function of the frequency of the oscillations.

The most detailed study of strain-thickening in concentrated dispersions was made by Boersma *et al.* (12). The systems investigated consisted of monodisperse silica or

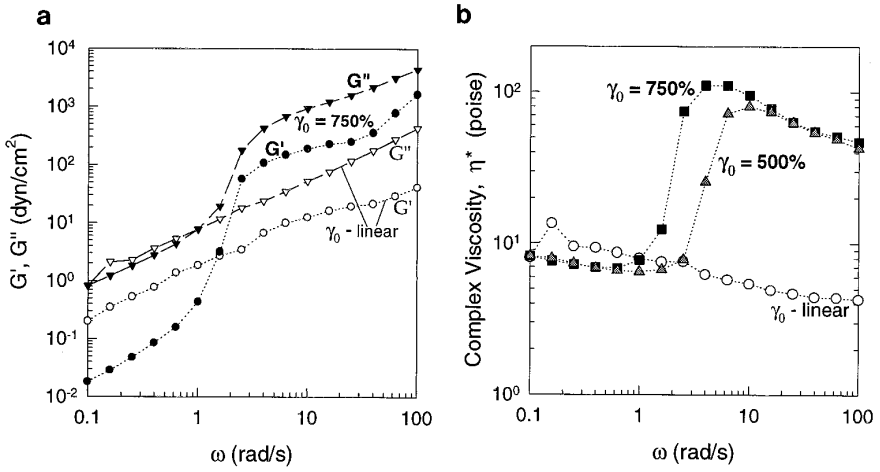

FIG. 6. Frequency sweeps for the 10% fumed silica suspension in PPG. In (a) the elastic G' and viscous G'' moduli are shown. The unfilled symbols correspond to the linear viscoelastic response, obtained at a sufficiently small strain within the linear regime. The data are identical to those shown in Fig. 2(a). The filled symbols represent the response at a strain amplitude of 750%. In (b) the complex viscosity, η^* is plotted as a function of frequency for three strain amplitudes: linear, 500% and 750%.

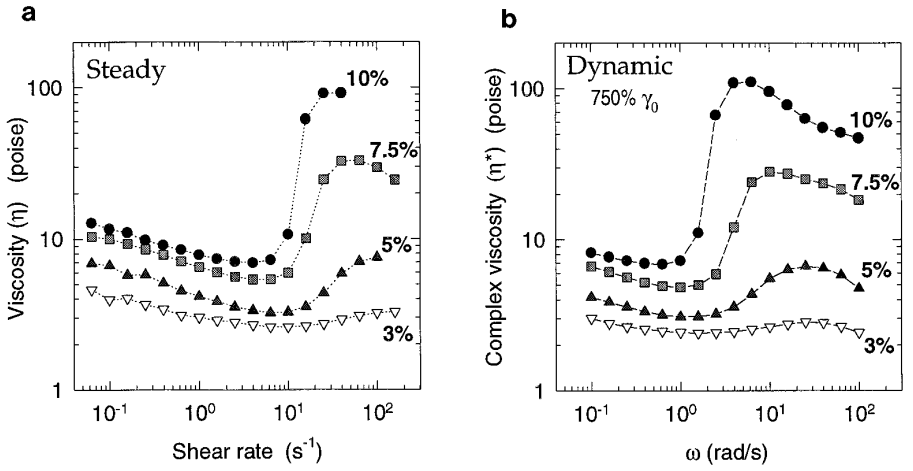

FIG. 7. Data for suspensions in PPG containing different weight fractions of fumed silica. In (a) the steady shear viscosity η is plotted as a function of shear rate. In (b) the complex viscosity η^* is plotted as a function of frequency for a strain amplitude of 750%.

glass particles suspended in a glycerol/water mixture. The particles were electrostatically stabilized by adjusting the pH. Suspensions at volume fractions exceeding 52% showed significant shear-thickening under steady shear as well as strain-thickening under oscillatory shear. Both strain sweeps as well as frequency sweeps were shown and are qualitatively similar to the data presented here in Figs. 5 and 6, respectively.

Shear-Thickening/Strain-Thickening at Different Concentrations

Fumed silica suspensions in PPG exhibit shear- and strain-thickening over a range of silica weight fractions (3–10%). Steady shear data (viscosity η vs. shear-rate) for these systems is shown in Fig. 7a, while their dynamic rheological response (complex viscosity η^* vs. frequency ω at a fixed strain of 750%) is shown in Fig. 7b. The increase in viscosity (η or η^*) due to shear-thickening is most appreciable at the higher concentrations. Important parameters characterizing the phenomena are the critical shear-rate $\dot{\gamma}_c$ corresponding to the onset of steady shear-thickening and the critical frequency ω_C at the onset of strain-thickening. Both these parameters are observed to decrease with concentration (Table 1).

TABLE 1
Critical Shear-Rates and Frequencies for Steady Shear-Thickening and Dynamic Strain-Thickening (obtained from Fig. 7)

Silica concentration (w/w) (%)	Critical Shear-rate at incipience of steady shear-thickening, $\dot{\gamma}_c$ (s^{-1})	Critical frequency at incipience of dynamic strain-thickening (at 750% strain), ω_c (s^{-1})
3.0	9.2	1.8
5.0	8.0	1.3
7.5	6.3	1.0
10.0	4.5	0.6

We can also plot the strain-thickening transition points—that is, combinations of strain amplitude and frequency at which the system begins to show strain-thickening—for each concentration. These transition points can be extracted from the $|G^*|$ vs. strain amplitude data (as shown in Fig. 5) or the η^* vs. frequency data (as in Fig. 6). A plot of the critical strain amplitude γ_C as a function of the critical frequency ω_C is shown in Fig. 8. We observe that γ_C decreases as ω_C increases, with two distinct ranges of behavior being apparent: at small frequencies, the decrease in γ_C is rapid, while at high frequencies, the curves asymptote toward a constant value of γ_C. The following equation can be used to model the data:

$$\gamma_C = \gamma_\infty + \frac{\dot{\gamma}_C^{dyn}}{\omega_C}. \qquad [1]$$

Equation [1] is similar to that used by Laun *et al.* (13) for their strain-thickening plots. The curves drawn through the points in Fig. 8 represent fits to the data using this equation. The values of the parameters γ_∞ and $\dot{\gamma}_C^{dyn}$ are shown in Table 2 and both parameters are found to decrease with concentration. The parameter γ_∞ represents the plateau strain at high frequencies, while $\dot{\gamma}_C^{dyn}$ is related to the behavior at low frequencies.

From Fig. 8 we find that at low frequencies, extremely high strain amplitudes are required for strain-thickening to be observed. In the low-frequency limit, the critical strain γ_C is inversely proportional to the critical frequency ω_C (Eq. [1]) and thus their product $\gamma_C\omega_C$ is a constant denoted by $\dot{\gamma}_C^{dyn}$ in Eq. [1]. In a dynamic experiment conducted at frequency ω and strain-amplitude γ_0, the product $(\gamma_0 \cdot \omega)$ corresponds to the maximum dynamic shear-rate. Thus, the pa-

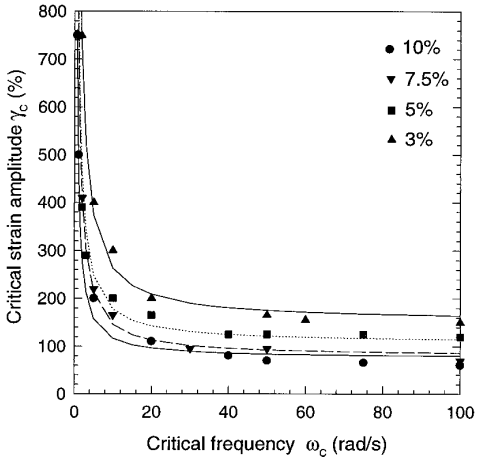

FIG. 8. Critical strain amplitude as a function of critical frequency, for fumed silica suspensions in PPG. Data shown in this plot were obtained from strain or frequency sweeps (as in Figs. 5 and 6) conducted for each silica concentration. The critical transitions correspond to the points when G^* or η^* show an upturn. The dashed lines drawn through the points represent fits to the data as given by Eq. (1).

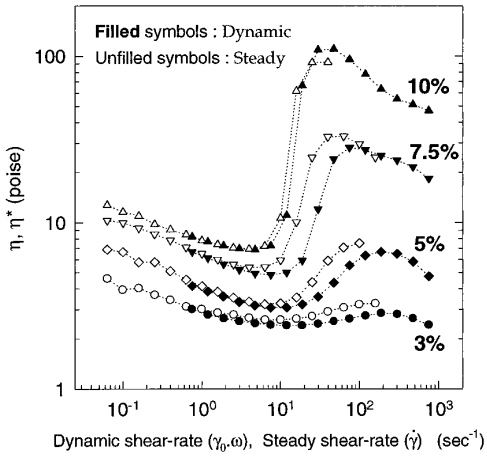

FIG. 9. Correlation of steady and dynamic data shown earlier in Fig. 7, using the modified Cox–Merz rule (Eq. [2]). The steady data (viscosity η vs. shear-rate) is reproduced unchanged from Fig. 7(a). The data for complex viscosity η^* is replotted against the maximum dynamic shear-rate, $\gamma_0 \cdot \omega$, where $\gamma_0 = 750\%$ is the strain-amplitude at which the frequency sweeps in Fig. 7(b) were all conducted.

rameter $\dot{\gamma}_C^{dyn}$ can be physically interpreted as a critical dynamic shear-rate.

We now examine the correlation between the two parameters $\dot{\gamma}_C^{dyn}$ and $\dot{\gamma}_c$ which mark the transition to strain-thickening and shear-thickening, respectively. Comparison of $\dot{\gamma}_C^{dyn}$ values in Table 2 with values of $\dot{\gamma}_c$ in Table 1 shows a strong correlation between them (within 20%), with both parameters decreasing with concentration. This suggests that the similarity between the steady and dynamic data in Figs. 7a and 7b, respectively, is not coincidental. The dynamic data in Fig. 7b corresponds to a deformation γ_0 of 750%. As the frequency is increased at constant deformation, the dynamic shear-rate ($\dot{\gamma}^{dyn} = \gamma_0 \cdot \omega$) increases, until at a critical frequency ω_C the dynamic shear-rate approaches its critical value ($\dot{\gamma}_C^{dyn} = \gamma_C \omega_C$) and the system shows strain-thickening.

The preceding analysis suggests that the dynamic shear-rate controls strain-thickening just as the steady shear-rate controls shear-thickening. To probe this relationship further, we have replotted the frequency sweep data from Fig. 7b as a function of the dynamic shear-rate $\gamma_0\omega$ (with $\gamma_0 = 750\%$). This is shown in Fig. 9, along with the steady rate sweeps for each concentration from Fig. 7a. Excellent overlap is observed at the 10% concentration, while the overlap progressively decreases at the lower concentrations. Similarly, we can also scale the data in Fig. 6b, which shows frequency sweeps (η^* vs. ω) for a 10% suspension at two different strain amplitudes, viz. 500% and 750%. When replotting the data against the dynamic shear-rate $\gamma_0\omega$, the value of γ_0 is different for each curve. The rescaled data are shown in Figure 10 along with the steady

TABLE 2

Parameters in Eq. [1] Describing the Variation of Critical Strain Amplitude γ_c with Critical Frequency ω_c (obtained from curve fits in Fig. 8)

Silica concentration (w/w) (%)	Plateau amplitude γ_∞ (%)	Critical dynamic shear-rate $\dot{\gamma}_c^{dyn}$ (s^{-1})
3.0	153.2	11.0
5.0	107.3	7.0
7.5	79.2	6.7
10.0	74.1	4.1

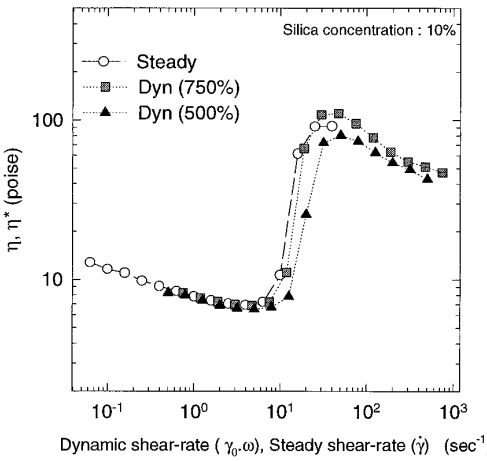

FIG. 10. Comparison of steady and dynamic data for a 10% fumed silica suspension. The steady data are shown in Fig. 7a and are reproduced unchanged. The dynamic data for the complex viscosity η^* as a function of frequency at two different strain amplitudes (500 and 750%) were shown in Fig. 6b. Here, η^* is replotted against the maximum dynamic shear rate $\gamma_0 \cdot \omega$, where γ_0 is the appropriate strain amplitude in the frequency sweep.

rate sweep for the same system, and the overlap observed is reasonably good. We have thus found the following correlation in our system, between the dynamic viscosities (obtained from a frequency sweep at a strain amplitude γ_0) and the steady shear viscosities

$$\eta^*(\gamma_0\omega) = \eta(\dot{\gamma})|_{\dot{\gamma}=\gamma_0\omega}, \quad [2]$$

where $\gamma_0\omega = \dot{\gamma}^{dyn}$ (i.e., the maximum dynamic shear-rate).

4. DISCUSSION

Validity and Significance of the Viscosity Superposition Rule

The preceding correlation between steady and dynamic viscosities has been proposed earlier by Doraiswamy *et al.* (21) for suspensions with a yield stress. The authors rigorously derived this relationship using a nonlinear rheological model and experimentally demonstrated its applicability for suspensions of silicon spheres in low-density polyethylene. They called it a *modified Cox–Merz rule* in view of its obvious resemblance to the well-known Cox–Merz rule for polymers which states that (22)

$$\eta^*(\omega) = \eta(\dot{\gamma})|_{\dot{\gamma}=\omega} \ . \quad [3]$$

Krieger (23) in a correspondence relating to the paper by Doraiswamy, pointed out a few significant differences between the two correlations. Firstly, the Cox–Merz rule relates the *linear* viscoelastic response of the system under oscillatory shear to the steady-shear properties. On the other hand, the modified Cox–Merz relationship compares the inherently *nonlinear* behavior under oscillatory shear with the steady shear properties. Thus the new rule is not exactly an extension of the original rule, and the similarity in names is rather misleading. Nevertheless, we propose that the modified Cox–Merz (or MCM) appellation be retained since it suggests a correspondence, albeit of a different kind, between steady and dynamic data.

A second point made by Krieger (23) concerns the applicability of the MCM rule. He suggested that the preceding correlation should apply to *any system* whose structural recovery time is longer than the period of oscillation. This comment assumes particular significance in the light of our study. As mentioned earlier, the MCM rule was originally derived by Doraiswamy *et al.* for suspensions exhibiting a yield stress. The mathematical formulation of the nonlinear model used by Doraiswamy requires the suspension to behave as a Hookean elastic solid below the yield stress σ_y and as a Herschel–Bulkley fluid beyond σ_y. In our case, the suspensions do *not* possess a yield stress, and the mathematical model used by Doraiswamy is clearly inapplicable. Nevertheless, our shear-thickening systems obey the same relationship between steady and dynamic behavior. Our findings thereby indicate a much broader applicability of the MCM rule, consistent with Krieger's hypothesis.

Krieger also predicts other interesting features in the rheology of systems that follow the MCM rule. He notes that the stress response of these systems, despite being highly nonlinear at the strains concerned, should nevertheless be sinusoidal (i.e., with negligible harmonic content) over the entire frequency regime. This is because the structure of the system would remain invariant throughout the cycle. This prediction is nicely borne out in our system, where the contribution of higher harmonics was found to be negligible. We should reiterate here that since the response is sinusoidal, we are indeed dealing with material properties rather than instrumental artifacts.

A correlation between steady and dynamic viscosities has never before been demonstrated for a shear-thickening dispersion. We have shown here that such a correlation indeed exists, as given by the modified Cox–Merz rule (Eq. [2]). We must emphasize that the predicted MCM rule is obeyed by shear-thickening suspensions only when the strain-amplitude in the frequency sweep is very high ($\gamma_0 \geqslant 500\%$). Under these conditions, the system assumes a degree of structure consistent with the maximum shear rate during each cycle, which is equal to $\gamma_0\omega$. Our suspensions do not show conventional Cox–Merz behavior, since the complex viscosity, η^* in the linear viscoelastic region *monotonically decreases* with ω (Fig. 6) and hence cannot be superposed with the steady viscosity.

Will the MCM rule be obeyed by other shear-thickening suspensions? We have reason to believe so, particularly for the systems investigated by Laun *et al.* (13) and Boersma *et al.* (12). Both have hinted at a correlation between the steady shear-thickening and the strain-thickening behavior of their systems, although they did not experimentally demonstrate this relationship. From the data reported, it appears likely that the steady and complex viscosities of their suspensions can be made to superpose using the MCM rule.

'Clustering' Mechanism for Shear-Thickening/Strain-Thickening

The preceding correlation between shear-thickening (steady) and strain-thickening (dynamic) show that the two phenomena are closely related in terms of their underlying mechanism. As mentioned in the introduction, there are two microstructural models that have been offered to explain shear-thickening. These are the order-disorder transition (ODT) theory and the cluster-formation theory (clustering for short). There is increasing indication that clustering is a more accurate and generalized model, with the ODT being a possible concomitant effect in many cases (5–9).

We believe that our results offer evidence in support of the clustering theory. We will, however, discuss first the

reasons why an order-disorder transition is not likely to occur in our system. The key feature of the ODT mechanism is the assumption that an ordered (layered) arrangement of particles exists at low shear rates. This ordering is caused by repulsive forces between particles and contributes to a reduced viscosity at these shear-rates (2, 3, 12). As the shear-rate is increased, the hydrodynamic forces on the particles increase, and at the critical shear-rate $\dot{\gamma}_c$, these forces induce disruption of the ordered state, thereby causing the viscosity to rise.

The formation of ordered particle layers is easy to visualize if the suspended particles conform to regular shapes, such as spheres or rods. In most of the classical studies on shear-thickening (1, 2, 4, 12), the particles in suspension were monodisperse spheres, stabilized either electrostatically or sterically. Thus, it is highly probable that the suspensions in these studies can show ordering at low shear rates. However, in our case, the primary flow units in the suspension are aggregates and not individual particles of silica. The silica aggregates are irregular, anisotropic structures (Fig. 1), which can be modeled as fractals (19). The aggregates may range in size from 0.1 to 0.5 μm and cannot be disrupted by shear into the primary particles (24). It seems unlikely that these irregular, polydisperse structures can be arranged into ordered layers at low shear rates.

In addition to particle geometry, the second key requirement for ordering is the presence of repulsive forces between particles. Note that the attractive forces between particles must be screened to ensure that a suspension is nonflocculated, and only such suspensions can exhibit shear-thickening. If there are strong colloidal repulsions between flow units, these forces can lead to the formation of ordered layers (2, 4). However, if the repulsive forces are weak, the disordering influence of Brownian motion can negate the ordering tendency. This was confirmed by simulations, where no evidence of ordering was found when the interparticle repulsion potential was weak (6). In our case, the silica aggregates in suspension are only weakly repulsive. The repulsion arises due to steric forces, which generally increase with molecular weight of polymer adsorbed (25). Since the polymeric continuous phase (PPG) is of low molecular weight, the steric effect due to adsorbed polymer will also be low. Therefore, an ordered state at low deformations is unlikely in our case.

We have shown that the ODT theory is not a reasonable model to explain our results. On the contrary, the clustering theory can account for the complex rheological behavior of our system. According to this theory, the shear-thickened (or strain-thickened) state is characterized by the presence of flow-induced clusters (5–9). At low shear rates, the silica aggregates in suspension are prevented from further association by weak steric repulsive forces and Brownian forces. As the shear-rate is increased, the hydrodynamic (shear) forces increase in magnitude, until at the critical transition, their level exceeds that of the repulsive interactions. At this point, clusters of aggregates are formed, as a result of which the viscosity (η or η^*) increases.

The reasons for the viscosity increase are twofold. Firstly, the formation of clusters leads to an increase in the effective volume fraction of disperse phase, due to occlusion of liquid within the clusters. The second factor concerns the shape of the clusters—the clusters are believed to be *elongated, nonspherical* structures (6). According to Bossis and Brady (6), the hydrodynamic stress will be proportional to the cube of the larger dimension situated in the plane of shear, implying that elongated clusters will contribute much more to the viscosity than spherical ones. Since we start out with a system of anisotropic aggregates (Fig. 1), we expect the anisotropy to be accentuated when clusters of such aggregates are formed under shear. Thus, the anisotropy of fumed silica units is expected to play a significant role in the shear-thickening behavior.

Note that the existence of a force balance at the transition point $\dot{\gamma}_c$ between hydrodynamic forces and interparticle repulsive forces is a common feature to both the ODT and the clustering models. The hydrodynamic force on the particles is typically approximated by a Stokes law-type expression, where the force F_D is directly proportional to the shear-rate $\dot{\gamma}$. For example, Boersma *et al.* (4) used the following expression which represents the hydrodynamic interaction between two spheres of radius *a*, separated by a distance *h*:

$$F_D = 6\pi\eta_0 a^2 \cdot \left(\frac{a}{h}\right) \cdot \dot{\gamma}. \qquad [4]$$

Here, η_0 is the viscosity of the dispersion medium. For shear-rates greater than $\dot{\gamma}_c$, the hydrodynamic forces predominate in the system.

Two Regimes of Strain-Thickening

The response of our suspension to *high-amplitude* oscillations is akin to that under steady shear. Under these conditions, the suspension behavior is governed by the maximum dynamic shear-rate, $\dot{\gamma}^{dyn} = \gamma_0\omega$, where γ_0 is the strain amplitude and ω is the frequency. The strain-thickening is controlled by the magnitude of the hydrodynamic force F_D which is proportional to the dynamic shear-rate. At a critical dynamic shear-rate ($\dot{\gamma}_C^{dyn} = \gamma_C\omega_C$) the hydrodynamic forces exceed the repulsive interactions and cause clusters to be formed. Thus the complex viscosity increases with dynamic shear-rate, mirroring the rise in steady viscosity with steady shear-rate (Fig. 9), and this also explains the MCM correlation (Eq. [2]). This behavior corresponds to the first regime of critical transitions (Fig. 8), where the critical dynamic shear-rate, $\dot{\gamma}_C^{dyn} = \gamma_C\omega_C$ is constant.

There also exists a second regime of strain-thickening

transitions in Fig. 8, which occur at constant strain-amplitude γ_∞ and relatively high frequencies. The behavior in this regime is quite different from that in steady-shear, and the response is not driven by the dynamic shear-rate alone. The ODT mechanism cannot be used to account for these results; however, we can explain them using a modified clustering mechanism. This, in fact, offers additional evidence in support of the clustering theory.

In the first regime, we expressed the condition for strain-thickening in terms of the level of shear (hydrodynamic) forces in the system. This implied that the hydrodynamic forces, on reaching a sufficient level, would inevitably cause the connection of aggregates into clusters (i.e., the aggregates would ''stick'' with a probability close to one). In the second strain-thickening regime, which occurs at high frequencies, we relax the latter condition and postulate that the ''sticking'' of aggregates on contact is no longer certain. This can be due to insufficient time of contact between aggregates at the high frequencies (note that a frequency of ω corresponds to a time scale $2\pi/\omega$).

We can represent this in a simplistic approach, by invoking a sticking probability $p(\omega)$ that is less than one and decreases with frequency ω. The strain-thickening transition in this regime can be considered to scale as the product of the shear force F_D and $p(\omega)$, while in the previous regime it scaled with F_D only, since $p(\omega)$ was equal to one. As the frequency increases, the probability of sticking $p(\omega)$ decreases. Hence a higher F_D is required to cause clustering. This is analogous to chemically limited aggregation, where particles stick only after many collisions (26). In the limit of very high frequencies, the sticking probability is postulated to decrease as $1/\omega$. In that case, the condition for strain-thickening becomes

$$\text{Strain-thickening transition} \sim [F_D \cdot p(\omega)]. \qquad [5]$$

Now, since,

$$F_D \sim \gamma_0\omega \text{ (i.e., the dynamic shear-rate)} \qquad [6]$$

and

$$p(\omega) \sim \frac{1}{\omega}, \qquad [7]$$

$$\therefore \text{ Strain-thickening transition} \sim \gamma_0\omega \cdot \frac{1}{\omega}$$

$$\sim \gamma_0 \text{ (independent of frequency).} \qquad [8]$$

This explains why at high frequencies, the strain-thickening transitions occur at a constant amplitude denoted by γ_∞ in Eq. [1]. The decrease in γ_∞ with concentration occurs because of the decrease in average interparticle distance with concentration.

Quantitative Characterization of the Disperse Phase

The preceding discussion has been largely qualitative, and we have not attempted to formulate a mathematical model for our system. In some previous studies, simple models have been used to predict critical shear-rates or other parameters (2, 4, 12). These models require quantitative information about the system such as the aggregate shape and size distribution as well as the effective disperse phase volume fraction. Due to the complicated nature of fumed silica suspensions, these parameters are not easy to obtain. The technique frequently used to determine size-distributions is dynamic light scattering (DLS); however, performing DLS on our suspensions will require considerable dilution, which would alter the very parameters we seek to measure. The same problem exists with different microscopic techniques, since the continuous phase will have to be removed before imaging.

The volume fraction of silica particles ϕ_s in our suspensions is very low (as calculated from bulk densities, it is 0.013–0.044, corresponding to the 3–10% w/w). Shear-thickening has never been observed at such low volume fractions (3). This puzzling aspect can be explained only by assuming that the effective disperse phase volume fraction ϕ_{eff} is much higher. The higher value of ϕ_{eff} over ϕ_s is due to a significant amount of liquid being occluded within the loosely packed silica aggregates (24). The open, loosely packed structure of silica aggregates is a consequence of their fractal nature. A fractal solid shows a lower density than a Euclidean solid; in effect it can be considered to have ''holes'' (27). In a fractal aggregate, these holes would be occupied by the liquid phase, and the entire structure would deform as a single entity, thereby increasing the effective volume fraction.

Note that a volume fraction of 0.013 (ϕ_s) for the 3% suspension, falls well within the limits of applicability of the Batchelor equation for suspension viscosity (25):

$$\eta_r = \frac{\eta}{\eta_0} = 1 + 2.5\phi + 6.2\phi^2 \quad \text{for } \phi < 0.2. \qquad [9]$$

This equation predicts the reduced zero-shear viscosity η_r of the suspension to be 1.0335, whereas the data in Fig. 7a (steady shear) indicates η_r to be about 3.33. The higher viscosity observed in practice indicates a much higher effective volume fraction ϕ_{eff} of solid phase. A crude estimate obtained using the Batchelor equation indicates ϕ_{eff} to be about 0.45, which is more than 30 times the value of ϕ_s. At the present time, we do not have more reliable estimates for the ϕ_{eff} parameter. Further characterization of our suspensions remains the focus of ongoing research.

5. CONCLUSIONS

Fumed silica suspensions in low molecular weight polypropylene glycol exhibit shear-thickening under steady flow and strain-thickening under oscillatory shear. Strain-thickening refers to the abrupt increase in the complex modulus G^* (or equivalently the complex viscosity η^*) and occurs at critical combinations of amplitude γ_C and frequency ω_C.

Strain-thickening at high strain amplitudes is qualitatively similar to steady shear-thickening. Data for the complex viscosity plotted as a function of dynamic shear rate $\gamma_0\omega$ can be superposed with viscosity—shear-rate data obtained under steady shear. The preceding correlation is a modified form of the Cox–Merz rule and has been found to be obeyed by Bingham plastic-like materials as well. At high frequencies, transitions to strain-thickening behavior occur at a relatively constant strain amplitude γ_∞, which is independent of frequency.

The combination of shear- and strain-thickening behavior can be explained through a clustering mechanism, which attributes the thickening phenomena to the presence of temporary, flow-induced clusters. These clusters are generated by the action of hydrodynamic forces on the silica aggregates. Under steady shear or under oscillatory shear at high amplitudes the connection of aggregates into clusters readily occurs. In the high-frequency limit of strain-thickening, the aggregates do not ''stick'' readily to form clusters. These qualitative arguments can be used to explain our results.

It is likely that every system that exhibits shear-thickening under steady shear would also show strain-thickening under oscillatory shear. The two phenomena have been simultaneously observed in a variety of systems. Moreover, it should be possible to explicitly correlate the two kinds of behavior, using the modified Cox–Merz rule. Our results also lend further support to the clustering theory for shear-thickening in suspensions.

ACKNOWLEDGMENTS

The authors gratefully acknowledge the support of the Department of Energy, Office of Basic Energy Sciences and NACE International for conducting this work.

REFERENCES

1. Hoffman, R. L., *Trans. Soc. Rheol.* **16,** 155 (1972).
2. Hoffman, R. L., *J. Colloid Interface Sci.* **46,** 491 (1974).
3. Barnes, H. A., *J. Rheol.* **33,** 329 (1989).
4. Boersma, W. H., Laven, J., and Stein, H. N., *AIChE J.* **36,** 321 (1990).
5. Boersma, W. H., Laven, J., and Stein, H. N., *J. Rheol.* **39,** 841 (1995).
6. Bossis, G., and Brady, J. F., *J. Chem. Phys.* **91,** 1866 (1989).
7. Brady, J. F., and Bossis, G., *J. Fluid Mech.* **155,** 105 (1985).
8. Bossis, G., Grasselli, Y., Lemaire, E., Meunier, A., Brady, J. F., and Phung, T., *Physica Scripta* **T49,** 89 (1993).
9. Bender, J. W., and Wagner, N. J., *J. Colloid Interface Sci.* **172,** 171 (1995).
10. Bender, J. W., Ph.D. thesis, Univ. of Delaware, 1995.
11. Collins, E. A., Hoffman, D. J., and Soni, P. L., *J. Colloid Interface Sci.* **71,** 21 (1979).
12. Boersma, W. H., Laven, J., and Stein, H. N., *J. Colloid Interface Sci.* **149,** 10 (1992).
13. Laun, H. M., Bung, R., and Schmidt, F., *J. Rheol.* **35,** 999 (1991).
14. Miller, R. R., Lee, E., and Powell, R. L., *J. Rheol.* **35,** 901 (1991).
15. Degussa Technical Bulletin No. 23, Degussa Corp., 1989.
16. Cab-o-sil Fumed Silica: Properties and Functions, Cabot Corp., 1987.
17. Khan, S. A., and Zoeller, N. J., *J. Rheol.* **37,** 1225 (1993).
18. Khan, S. A., Baker, G. L., and Colson, S., *Chem. Mater.* **6,** 2359 (1994).
19. Forsman, J., Harrison, J. P., and Rutenberg, A., *Can. J. Phys.* **65,** 767 (1987).
20. D'Haene, P. D., Mewis, J., and Fuller, G. G., *J. Colloid Interface Sci.* **156,** 350 (1993).
21. Doraiswamy, D., Mujumdar, A. N., Tsao, I., Beris, A. N., Danforth, S. C., and Metzner, A. B., *J. Rheol.* **35,** 647 (1991).
22. Cox, W. P., and Merz, E. H., *J. Polym. Sci.* **28,** 619 (1958).
23. Krieger, I. M., *J. Rheol.* **36,** 215 (1992).
24. Eisenlauer, J., and Killman, E., *J. Colloid Interface Sci.* **74,** 108 (1980).
25. Russel, W. B., Saville, D. A., and Schowalter, W. R., ''Colloidal Dispersions,'' Cambridge University Press, Cambridge, 1989.
26. Rouw, W. P., and de Kruif, C. G., *Phys. Rev. A* **39,** 5399 (1989).
27. Feder, J., ''Fractals.'' Plenum Press, New York, 1988.